average nodding frequency of the axis of symmetry appears to be relatively unaffected by changes in the inertia or solar parameter.

The effect of the spin parameter σ on the librational behavior is indicated in Fig. 2b. Here again, critical values of the spin parameter exist for which the satellite tumbles over. A large value of the spin parameter, in general, leads to smaller coning angles as anticipated.

Figure 2c shows the influence of the orbital eccentricity on the attitude motion. In general, higher values of the orbit eccentricity result in larger amplitude motion. Unlike the effect of the inertia and the spin parameters, no resonant behavior is noticed for the typical system parameters considered here.

The influence of the significant orbital parameters, such as i, ϕ, ω, and the solar aspect ratio G, on the satellite performance was also investigated. The amplitude of oscillation was found to reduce gradually with an increase in the orbital inclination from the ecliptic (Fig. 2d). Changes in the solar aspect angle ϕ, which depends upon the location of the line of nodes and the apparent position of the sun, did not affect the amplitude of librations and their frequency. The influence of the perigee position ω and the solar aspect ratio G was also found to be insignificant.

From design considerations, it would be desirable to assess the magnitude of the solar pressure torque that a satellite can withstand without exceeding the permissible bound of libration as governed by the mission requirements. This bound then would establish a criterion for stability. Here, the stability limit is purposely taken as a large value of $\Phi = \pi/2$ to emphasize the vulnerability of the satellite's performance to the solar pressure torque.

Figure 3a shows a typical stability chart for librational motion in a circular orbit with the solar radiation pressure as the only excitation. The equations of motion (3) were integrated over 15–20 orbits for a range of values of satellite inertia and spin parameters. The resulting information about the maximum amplitude of the coning angle Φ_{max} was then condensed in the form of the stability plots in the $I-\sigma$ space. The analysis shows that in addition to the main stable region for high inertia parameter values, there also exist small isolated stable areas. However, there are substantial unstable regions even for positive spin or large inertia parameters. It is observed that the stable areas reduce drastically, as expected, with an increase in the value of the solar parameter.

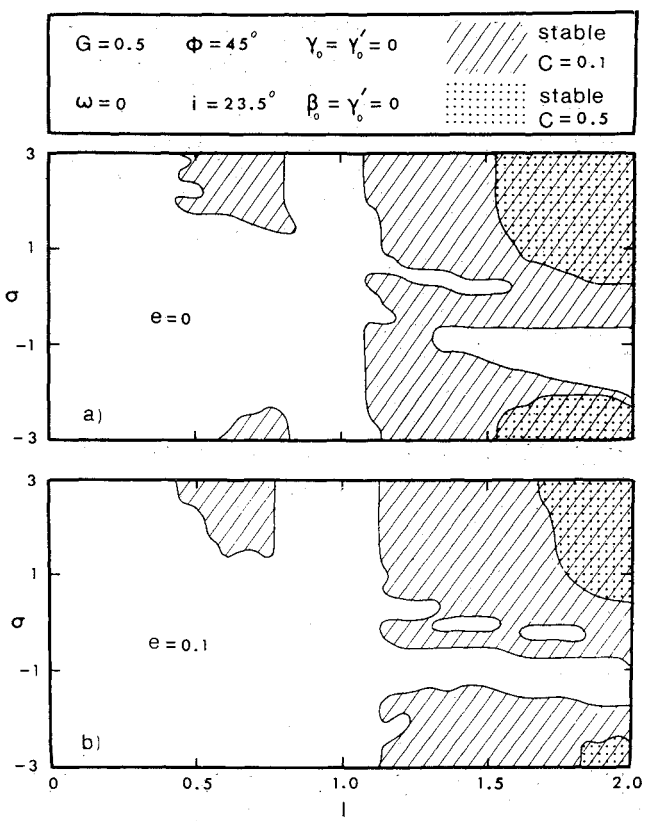

Fig. 3 Typical stability charts showing adverse influence of the solar radiation pressure. a) $e = 0$; b) $e = 0.1$.

The effect of the orbital eccentricity on the stability of librational motion is presented in Fig. 3b. An increase in orbital eccentricity further enhances the destabilizing influence of the solar pressure. The effect appears to be more pronounced for satellites spinning in a direction opposite to that of the oribital motion.

Of particular significance is the conclusion that the value of C as small as 0.5, which would physically correspond to $\varepsilon = 0.1$ ft for INTELSAT IV category of satellites ($I \simeq 0.7$) at synchronous altitude, causes the satellite to tumble over. The critical values of eccentricity, inertia, and spin parameters would only accentuate this behavior. Of course, in actual practice, a higher spin rate and/or active control system would counter this tendency. Nevertheless, the analysis clearly brings out the fact that the solar parameter C is of the same importance as I, σ, and e in the design of the satellite attitude control system.

Reference

[1] Modi, V. J. and Pande, K. C., "On the Solar Pressure Excited Librations of Spinning Axisymmetric Satellites," Mechanical Engineering Rept. ME 73-25, Feb. 1973, Univ. of British Columbia, Vancouver, Canada.

Example of Dynamic Interference Effects between Two Oscillating Vehicles

K. J. ORLIK-RÜCKEMANN* AND S. IYENGAR†
National Aeronautical Establishment,‡ Ottawa, Ontario, Canada

Nomenclature

C_m = (pitching moment with static interference)/(qSl)
$C_{m\theta}$ = $\partial C_m/\partial\theta$, static pitching moment derivative
$C_{m\dot\theta}$ = $\partial C_m/\partial(l\dot\theta/2V)$, pitch damping derivative
$C_{m\theta}'$, $C_{m\dot\theta}'$ = effective derivatives, with dynamic interference
G, H = dynamic interference factors (for synchronous oscillation $G = C_{m\theta}'/C_{m\theta}$ and $H = C_{m\dot\theta}'/C_{m\dot\theta}$)
i = difference between the incidence of the orbiter and that of the booster
I_{YY} = moment of inertia about pitch axis
= reference length of each vehicle
q = dynamic pressure
S = reference area of each vehicle
Δx, Δz = longitudinal and vertical separation, respectively, between the centers of gravity, see Fig. 3

Presented at the AIAA 2nd Atmospheric Flight Mechanics Conference, Palo Alto, Calif., September, 11–13, 1972. Received April 4, 1973; revision received May 11, 1973. The assistance of the NASA Langley Research Center in providing the initial computer program is gratefully acknowledged.

Index category: Aircraft Handling, Stability, and Control.

* Head, Unsteady Aerodynamics Laboratory. Associate Fellow AIAA.

† Research Associate.

‡ A division of the National Research Council of Canada.

V = velocity
α = mean angle of attack of the orbiter
$\theta, \dot{\theta}$ = angular deflection in pitch and angular rate in pitch, respectively
$\bar{\theta}$ = amplitude in pitch
ϕ = phase angle between motions of the orbiter and the booster (orbiter leading)
ω = instantaneous frequency

Subscripts
O, B = orbiter and booster, respectively

Introduction

THE dynamic interference between two vehicles flying in the vicinity of each other may be defined as the interference on one of the vehicles caused by the other vehicle when it performs some motion (such as pitch oscillation) with respect to a system of coordinates moving with the c.g. of the first vehicle. One example of a situation when the dynamic interference may be large is the abort separation of the early fully reusable version of the space shuttle. It has been shown[1] that the pitch damping of a space shuttle orbiter could be dramatically changed by the dynamic interference from an oscillating booster in close proximity. It was demonstrated that when the two vehicles oscillated with the same frequency, the pitch damping of the orbiter could vary between +13 and −8 times its interference-free value, depending on the phase angle between the two motions. So far, however, no information has been available as to the significance of the dynamic interference on the flight behavior of any of the component vehicles. In this Note a method is presented by means of which the dynamic-interference effects on both the dynamic and static pitching-moment derivatives can be accounted for in a flight mechanics analysis of an abort-separation maneuver. It is shown that it is indeed realistic to expect that the two vehicles may in some cases oscillate with the same frequency shortly after separation and that, when this happens, fully measurable and nonconservative effects on the orbiter flight may occur. Although the present results refer specifically to the abort separation of a fully reusable delta-wing shuttle, the conclusions may be of interest also for the current, partially reusable shuttle and, indeed, for many other situations involving two vehicles flying in close proximity.

Analysis

In the investigation of Ref. 1 the pitching-moment derivatives were measured on an oscillating orbiter in the presence of a booster that was either stationary (causing static interference) or performing an oscillatory motion (causing dynamic interference). The results, which so far have been obtained only at Mach 2 and only for one relative position of the centers of gravity of the two vehicles, are presented here as dynamic-interference factors G and H, which are plotted in Fig. 1 as functions of the phase angle between the motions of the two vehicles. By curve-fitting these functions, analytical expressions for G and H were obtained. For example, for an amplitude of 1.9° of both vehicles and for the single set of separation parameters investigated ($i = \alpha = 0°$, $\Delta x/l = -0.06, \Delta z/l = 0.19$), we had

$$G = 0.83 - 0.39\cos\phi \quad (1)$$

$$H = 2.45 + 15.0\sin(\phi + 13°) \quad (2)$$

The analysis was based on the NASA Langley Research Center (LRC) Abort Separation Program.[2] This program consists of 12 simultaneous equations of motion (6 for the orbiter and 6 for the booster) and a matrix summarizing the experimentally obtained static interference data for the aerodynamic coefficients of both vehicles in the plane of symmetry. To account for the dynamic interference effects, effective derivatives $C_{m\theta}'$ and $C_{m\dot{\theta}}'$ had to be introduced. When the two motions were synchronous, the simple relations

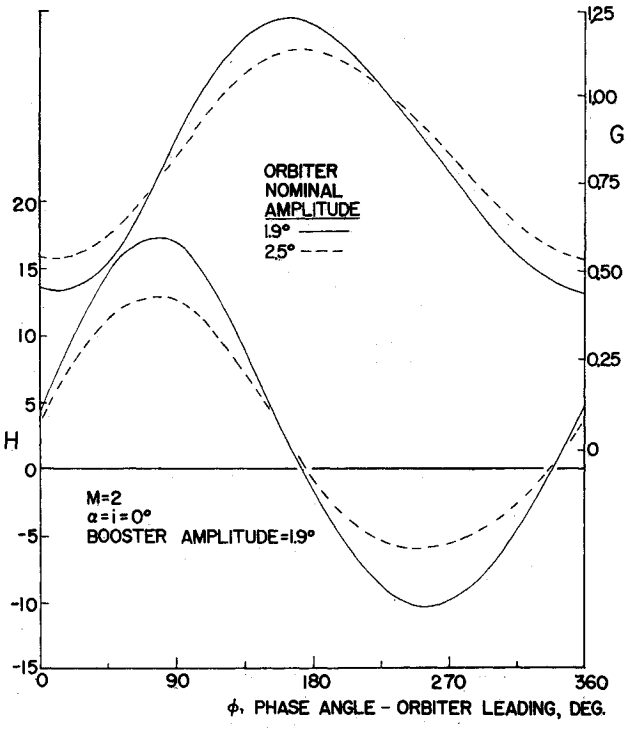

Fig. 1 Dynamic interference factors G and H (based on data of Ref. 1).

$C_{m\theta}' = GC_{m\theta}$ and $C_{m\dot{\theta}}' = HC_{m\dot{\theta}}$ could be directly used. In the general case of the frequencies of the two vehicles being unequal, a cushioning factor

$$F = (\omega_O/\omega_B)^n \text{ [where } |n| > 1, \text{ such that } F \leq 1] \quad (3)$$

was employed to provide for a gradual introduction of the dynamic interference effect. The effective derivatives then were

$$C_{m\theta}' = C_{m\theta}[1 + (G - 1)F] \quad (4)$$

$$C_{m\dot{\theta}}' = C_{m\dot{\theta}}[1 + (H - 1)F] \quad (5)$$

Although it is difficult to determine the exponent in Eq. (3) experimentally, the general form of Eqs. (4) and (5) does agree with experimental observations and a value of $|n|$ between 2 and 4 seems to provide a realistic representation of the variation in $C_{m\theta}'$ and $C_{m\dot{\theta}}'$ with varying frequencies of the two vehicles. In the present analysis it was assumed that $|n| = 2$. Because of the limitations of the experimental data available at the present time, the dynamic interference effect was considered only for the derivatives $C_{m\theta}'$ and $C_{m\dot{\theta}}'$ of the orbiter and only due to the pitching motion. In a real case, the corresponding dynamic interference on the booster derivatives and the dynamic interference due to the simultaneous plunging and rolling motions may also be important. As for the derivatives with static interference only, $C_{m\theta}$ was allowed to vary in accordance with the matrix, while $C_{m\dot{\theta}}$ was assumed to be approximately independent of the separation parameters Δx, Δz, and i, which was consistent with experimental data.[1]

The method of analysis is described by the block diagram in Fig. 2. The initial conditions chosen had to be consistent with the assumed values of amplitudes, frequencies and phase. The occurrence of collision, if any, was detected by a separate subroutine. Since in the LRC matrix the aerodynamic data were given in the form of instantaneous coefficients, the equivalent static pitching derivatives $C_{m\theta}$ for both the orbiter and the booster, had to be determined from

$$C_{m\theta} = (C_m)_{\text{matrix}}/(\theta - \theta') \quad (6)$$

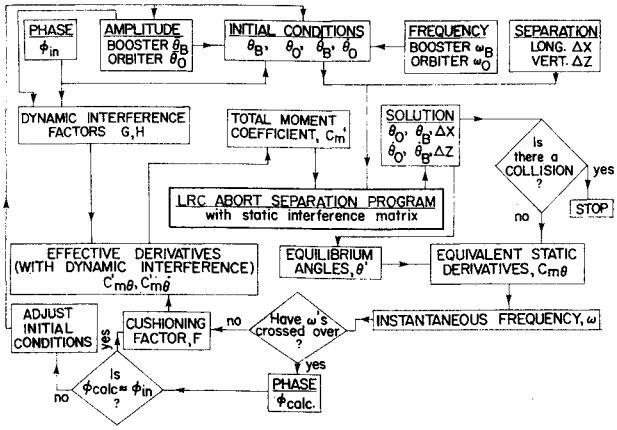

Fig. 2 Block diagram of the present method of analysis.

where the equilibrium angle θ' was obtained as the angle at which $(C_m)_{\text{matrix}}$ was zero. Instantaneous frequencies for both vehicles were introduced as

$$\omega = [(C_{m\theta} qSl)/I_{YY}]^{1/2} \tag{7}$$

It was found that these frequencies were strong functions of the relative position of the two vehicles and could vary sigficantly during a separation maneuver. A subroutine was developed for the recognition of the crossing-over of the frequencies of the two vehicles and for the determination of the phase angle at that moment; this calculated phase angle ϕ_{calc} was then compared with the value ϕ_{in} initially assumed.

After the determination of the instantaneous effective derivatives, the total pitching moment coefficient C_m' was calculated from

$$C_m' = (\theta - \theta')C_{m\theta}' + (\dot{\theta}l/2V)C_{m\dot{\theta}}' \tag{8}$$

This value was then used in the next step of the program replacing the value previously obtained on the basis of static interference data for that particular set of separation parameters. It should be noted that the first term on the RHS of Eq. (8) was equal to $[1 + (G - 1)F](C_m)_{\text{matrix}}$.

Results

The computations were performed for several sets of initial separation conditions, as given by the initial values of Δx and Δz, and by the initial angular deflections and angular velocities of the two vehicles. By means of a simple trial and error procedure the initial conditions were also made compatible with the frequency, amplitude and equilibrium data obtained from the first few steps of the computation, and also served to obtain the phase information for the first frequency crossover (if any). All computations pertained to an abort separation maneuver at Mach 2 at an altitude of 60,500 ft. In the majority of cases the separation either went smoothly, with the two vehicles flying gradually apart, or led to a rapid collision, without the frequencies crossing-over and, therefore, without establishing conditions necessary for the manifestation of the dynamic interference effects.

A few cases were found, however, where the frequencies of the two vehicles did cross over, and the flight histories of both vehicles were then studied in detail, using partly the present method (with dynamic interference) and partly the unmodified LRC program (with static interference only). An example of such a case is given in Fig. 3, for the following initial conditions: $\theta_O = -0.35°$, $\theta_B = -3.00°$, $\dot{\theta}_O = -0.093$ rad/sec, $\dot{\theta}_B = -0.131$ rad/sec, and $\phi_{\text{in}} = 315°$. The inclusion of dynamic interference increased the initial amplitude of the orbiter pitching oscillation from 8° to 14° and at the same time changed the

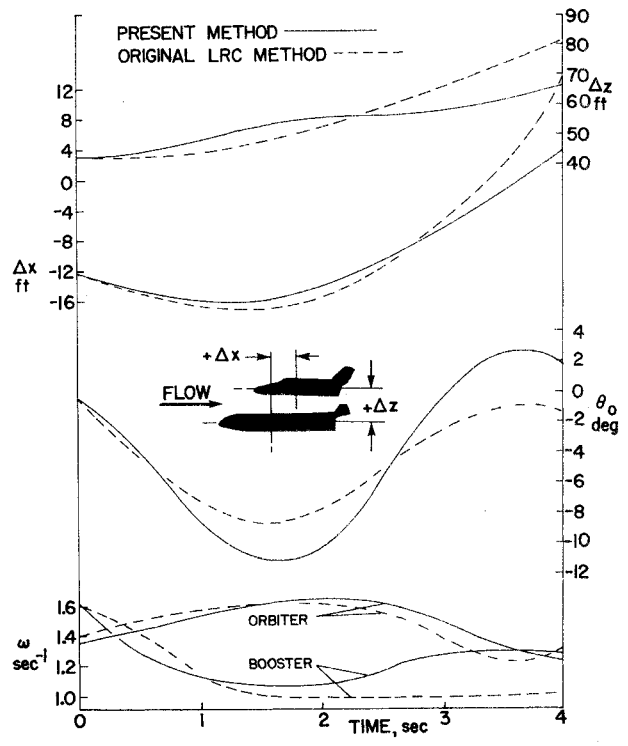

Fig. 3 Orbiter incidence, orbiter and booster frequencies, and longitudinal and vertical separation distances for the first 4 sec after separation.

angular motion from converging to diverging. The present method indicates that after the initial crossover at $t = 0.4$ sec the two frequencies crossed over again at $t = 3.7$ sec and then remained very close, increasing the possible impact of dynamic interference. At the same time the present method gives considerably smaller variations in Δx and Δz (indicating that the two vehicles remained close together for a longer period of time) than can be predicted without taking dynamic interference into account.

Summary and Conclusions

The principal message of this paper is that the mutual static interference between two vehicles flying in the proximity of each other may cause their instantaneous frequencies to become nearly the same, and that whenever this happens (even if only for a short time) a strong and hitherto unaccounted-for dynamic interference may occur which could alter the subsequent flight history of one or both of the companion vehicles. This was demonstrated by considering the dynamic interference of the booster on the flight behavior of the orbiter in a hypothetical abort-separation case of the fully reusable space shuttle. The study was of an exploratory character, was based on very sparse experimental data and involved certain simplifications. The results, therefore, should be considered in a qualitative, rather than quantitative, sense.

References

[1] Orlik-Rückemann, K. J., LaBerge, J. G., and Hanff, E. S., "Supersonic Dynamic Stability Experiments on the Space Shuttle," *Journal of Spacecraft and Rockets*, Vol. 9, No. 9, Sept. 1972, pp. 655–660.

[2] Decker, J. P., Blackwell, K. L., Sims, J. L., Burt, R. H., Strike, W. T., Jr., Andrews, C. D., Baker, L. R., Jr., and Rampy, J. M., "Abort Separation of the Shuttle," TM X-2509, Feb., 1972, NASA, pp. 1105–1164.